



Fermi National Accelerator Laboratory

TM-1680

**Study of Drift Tube Resolution
Using Numerical Simulations**

Mark C. Lundin
*Fermi National Accelerator Laboratory
P.O. Box 500
Batavia, Illinois 60510*

October 10, 1990



October 10, 1990

Study of Drift Tube Resolution Using Numerical Simulations

MARK C. LUNDIN

Fermi National Accelerator Laboratory P.O. Box 500 Batavia, Illinois 60510

ABSTRACT

The results of a simulation of straw tube detector response are presented. These gas ionization detectors and the electronics which must presumably go along with them are characterized in a simple but meaningful manner. The physical processes which comprise the response of the individual straw tubes are broken down and examined in detail. Different parameters of the simulation are varied and resulting predictions of drift tube spatial resolution are shown. In addition, small aspects of the predictions are compared to recent laboratory results, which can be seen as a measure of the simulation's usefulness.

1. Introduction

This study is accomplished in two parts. In the primary part, GEANT¹ was used to simulate the straw tube *superlayers* whose geometry is shown in Fig. 1 to be an 8x75 array of drift tubes arranged in a hexagonal close-packed structure which will serve in a tracking capacity for the Bottom Collider Detector². The Monte Carlo events generated with this simulation can then be combined with a careful parameterization³ of gas ionization, electron-ion mobility, and amplification and shaping of the resulting individual straw tube signal. The purpose of this secondary portion of the simulation is, of course, to produce information regarding probable straw tube detector response. The latter parts of this characterization are now shown here to demonstrate the numerical production of straw tube resolution predictions for various discriminator trigger levels and detector parameters. Results from variations in the basic properties of the detector's gas and electronics characterizations are compared to each other in order to give some idea about the contributions of each component to detector resolution results. This information is intended for use in a variety of areas, the primary being the construction and testing of track fitting algorithms for the proposed Bottom Collider Detector.

2. Physical Characteristics of the Straw Tube Detector

Straw tubes are simple gaseous drift chamber detectors whose layout is shown in Fig. 2. Due to their geometry and proximity to each other it's natural to expect that they will provide added resolution as a detector. In this study, a simulation parametrizes the straw tubes as 4mm diameter mylar cylinders, 2 meters in length. The mylar tube's inner surface is covered with a 0.31 micron thick coating of aluminum, which acts as the tube's cathode. For this study we have parametrized argon-ethane (50%/50%) at various pressures. A wire runs down the tube's central axis and acts as the anode. A voltage is placed on the wire which creates an electric field inside the tube itself. Any radiation penetrating the straw tube under these conditions will create a certain number of electron-ion pairs. The radial electric field will accelerate the electrons towards the anode and the ions towards the cathode, or aluminized outer wall of the cylinder.

3. Limitations Imposed on the Straw Tubes

Our Monte Carlo supplies a particle with a random momentum vector. The particle passes through the gas which is declared to be a sensitive volume. However, for this study, a second simulation has been created which only considers the case of a generic particle track at various pre-determined distances from the central anode wire of the straw tube. The simulation considers many tracks with precisely the same distance of closest approach (DCA) to the central anode wire. After this has been accomplished, the simulation moves the track so that its DCA is larger than previously considered, until finally, the track has traveled from very near the anode wire (nearly becoming a diameter cord) until it is nearly tangent with the cathode at the edge of the straw tube cylinder wall.

One could parametrize the number of ion-electron pairs created for a given energy loss and use this information to simulate the drift of individual electrons and positive ions into the anode. Generally, all that is required is the energy of the particle in question along with the type of gas under investigation. In this way, the occurrence of ionizing reactions can be approximated through statistical means. However, we will only be considering detector response to the gross ionization clusters which result from particle energy loss. We will not try to simulate the number of ions or charge that these clouds are comprised of. Once the number and geometry of the ionization clusters for a given particle track have been chosen, we will apply a random amplification factor to account for the number of ionizing reactions occurring before the electrons and positive ions reach the anode. Later, careful consideration will be given to various discriminator trigger thresholds and levels will be chosen based on the mean number of ionization clusters which were collected before a trigger occurred.

Ionization events are randomly distributed along the particle track according to a Poisson distribution with some mean number of events per cm. This value is taken to be 25.2 for ArC_2H_6 at STP. This is an interpolation between that of 29.4⁴ for argon and 21⁵ for ethane. These ionization events are randomly placed along the particle track such that the average distance between created ionization clusters remains constant for a given DCA, and also between tracks of differing DCAs.

The electrons which make up the events drift radially towards the wire in an electric field. At this point an assumption is made that this field is sufficient in intensity to quickly accelerate the ion clouds to their saturation velocity. It is further assumed that field intensity isn't so great that it might reduce ionization

cluster drift velocity as a result of cascading effects. At the same time that the electron clusters drift towards the anode wire, there is a radial diffusion effect which we have characterized by a gaussian distribution with $\sigma=0.5\sigma_t$, where σ_t is taken to represent the transverse diffusion which varies as the square root of the radial distance .

There must be an accounting for the statistical variance in the charge which each ionization cluster holds, along with the secondary and tertiary ionizations which occur during the cluster drift towards the straw tube anode. As a result, at the wire, each electron is independently amplified by a random factor A_i which is distributed according to:

$$P(\eta) = \frac{3}{2}\eta e^{-\frac{3\eta}{2}}, \eta = \frac{A_i}{\bar{A}}$$

The tube acts as a transmission line driven by a current source resulting in a voltage pulse which is given by

$$V(t) = \frac{A_i}{(t_o + t)}, t_o = 1ns$$

for a typical drift type chamber. Electronic amplification of this signal is characterized by a rise time, t_r , followed by a long fall time. This gives for the final output signal a voltage:

$$V(t) = \frac{A_i}{t_r} \ln\left(1 + \frac{t}{t_o}\right), t < t_r$$

$$V(t) = \frac{A_i}{t_r} \left(\ln\left(1 + \frac{t}{t_o}\right) - \ln\left(1 + \frac{(t - t_r)}{t_o}\right) \right), t > t_r$$

Where $V(t)$ is the resulting voltage based on the chosen amplification factor. Amplifiers generally have some variable rise time. This is simulated by choosing

a random number distributed according to the positive half of a gaussian, whose mean is the fastest rise time advertised by the manufacturer and whose sigma is one third to one half of the manufacturer's advertised slowest amplifier rise time.

A discriminator cut is applied to the final signal, which is the sum of all ionization cluster pulses delayed relative to each other by the cluster arrival times at the sense wire.

4. Results

Fig. 3 shows a scenario in which the amplifier rise time is taken to be 10 ns, and the longitudinal diffusion is characterized by the product of $120\mu\text{m}$ and the square root of the distance travelled by the electron cluster. The figure displays a variety of discriminator trigger levels ranging from the ridiculously hopeful to the extremely conservative (bottom to top, respectively). So, for instance, in Fig.3, from bottom to top, each line represents progressively higher discriminator level settings which are noted in the figure caption. Each line shows that detector's resulting resolution values as a function of track DCA. The error bars displayed are simply statistical in nature and not in any way experimental. Their magnitude is inversely proportional to the square root of the number of particle tracks considered for that particular resolution value. The resolution value itself is taken to be the r.m.s. value of the normal distribution of the difference between divined and actual particle track distances of closest approach.

In order to gauge the appropriateness of the curve shown, Fig. 4 displays a histogram of the mean number of ionization clusters required for the discriminator to trigger at the levels in Fig.3. The histogram is assembled from the statistics of 2000, 1 track events averaged over DCAs which vary from very near to, to

very far from, the anode. No attempt is made to divine the number of electrons which each cluster represents.

Clearly, the resolution is quite sensitive to the discriminator level choice, especially in the region very near the wire. The mid region of the DCA plot, between the anode and the cylinder wall, shows a reduction in sigma. Near the straw tube anode, resolution is poor because of the small section of track that is actually near the wire. When a track is characterized as having a small DCA, the wire *may* see one or more ionization clusters which were created, by chance, very near the anode, but the majority of clusters will have to come from much greater distances (by up to 2 or 3 orders of magnitude) than the track DCA. When the track DCA is increased, the ambiguity due to this effect rapidly decreases. In the case of tracks whose DCA point is further out, near the cathode, resolution also becomes sensitive to diffusion and statistical effects. This is especially applicable to cases in which a track's DCA point is near the straw tube cylinder's outer wall where the detector efficiency is likely to drop below 80%.

Of course, this information does not take into account the detector inefficiencies due to particle tracks which, for various reasons failed to trigger the discriminator at a given level. This would be the result of having a low number of ionization clusters created along the particle track, failure of a given number of clusters to arrive within a sufficient time proximity to each other, an overly conservative discriminator setting or just a combination, to some extent or another, of all three conditions. Fig. 5 shows the detector efficiency for the parameters listed above, from a near zero DCA at the straw tube anode, to a track DCA point which is very near the tube cathode.

4.1. RESULTS OF VARYING THE AMPLIFIER RESPONSE TIME AND LONGITUDINAL DIFFUSION FACTOR

Fig. 6 shows a given drift tube parametrization for which different factors were used to describe the longitudinal diffusion which takes place as the ionization clusters drift towards the anode. Clearly, the diffusion representation in the simulation has a large impact on the resulting resolution values, especially when considering particle tracks with larger DCA's. In addition, amplifier rise times are altered to show that there is some loss in resolution caused by a slower amplifier. However, this effect begins to disappear in the case of greater track DCA's, especially when considering drift parameterizations in which there is relatively less longitudinal diffusion (as in the lower two curves).

4.2. COMPARISON TO LABORATORY RESULTS

Increasing the straw tube drift-chamber's inner radius and slightly altering the tube anode diameter allows the comparison of simulation results to recent laboratory results. Using a pulsed N_2 Laser, Lu et. al.⁶ have investigated various aspects of the timing properties for the proportional drift tube.

Spatial resolution data was obtained by firing an N_2 laser, with 337-nm pulse, through the window of a pressurized, aluminum, 7.67-mm-diameter, cylindrical drift chamber. The laser pulse was focused on the inner wall of the tube after passing through a 1-mm-diameter hole in the wall. The hole is offset by 1mm from the anode of the chamber. At least 90% of recorded events were initiated by single photoelectrons. At 1 atmosphere, 2000 volts were placed on the chamber anode (which was 1 mil in diameter⁷) and voltage was increased at higher drift tube operating pressures in order to maintain a constant gas gain. As a result

of this variance the gas drift velocity was kept at a relatively constant function of the electric field. Fig. 7 shows the electric field value as a function of radius with 1600 volts across the anode wire. Also shown on this figure is the resulting drift velocity as transcribed from known data concerning electron velocity as a function of electric field⁸. Since the drift velocity does not vary significantly from 5 cm/ μ sec, we assume this to be constant (for the sake of our simulation) for all ionization clusters regardless of their origin or location within the chamber.

Lu et. al. used a LeCroy TRA402 preamplifier with the drift-tube, whose rise time is characterized by a minimum of 3 ns but which could be as large as 7 ns. For purposes of the numerical simulation, this rise time was characterized by the absolute value of a random number added to a constant 3 ns. The random number was normally distributed with a mean of 0 and standard deviation of 1.5 ns.

The simulation's longitudinal diffusion factor was taken to be $\sigma = 167.5 \mu\text{m}\sqrt{\text{Distance}(\text{cm})}$. This was arrived at by averaging the experimental results of F.Pius⁹ (210 $\mu\text{m}/\sqrt{\text{cm}}$) and Jean-Marie et al.¹⁰ (125 $\mu\text{m}/\sqrt{\text{cm}}$) for ArC_2H_6 (50/50).

Spatial resolution values for this configuration as a function of pressure are shown in Fig. 8. The data points represent resolution values for single photoelectron events (with 90% probability) drifting from the inner wall of the drift-tube cylinder to the anode wire. To accomplish this, a variety of trigger thresholds were simulated simultaneously. The level chosen was the highest possible threshold level for which 90% or more of the events registered and also required only one ionization cluster for a trigger to occur. Generally, the discriminator trigger threshold level needed to accomplish this was between 10^{-1} and 10^{-2} volts.

Also on this figure is displayed the *simulated* spatial resolution values for particle tracks whose DCA point was within $0.1 \mu\text{m}$ of the drift tube cylinder inner walls.

5. Conclusions

Comparisons between the experimental data and the numerical simulation method seem to be quite encouraging. However, at this time other experimental scenarios are being compared with simulation values to insure that the numerical simulation method described here is a plausible one. Errors in spatial resolution values could be the result of several different possibilities. One phenomenon which should be investigated is the exponential decrease in resolution near the tube wall due to the drift tube's cylindrical geometry. It is also possible that a more careful simulation in which the electron-ion pairs themselves (as opposed to the gross ionization clusters) were modeled, could raise the efficiency of the drift tube near the cathode in addition to flattening out and raising the resolution predictions. This simulation is one in which a gross parameterization was chosen over a more detailed version so that the simulation would require less running time.

6. Acknowledgements

C. Lu and K.T. McDonald are recognized for their help, advice and interest in this work. Acknowledgement should also be given to the BCD software tracking group members for their time and criticisms, especially Linda Stutte, Paul LeBrun and Jean Slaughter whose advice and patience was invaluable.

In addition, this work was supported by the Loyola University of Chicago's mathematics and computer science department and the Fermi National Acceler-

ator Laboratory Particle Detector Group. This work was also supported by the United States Department of Energy.

REFERENCES

1. GEANT3 Document, CERN DD/EE/84-1 (September, 1987), HITS 001-2.
2. Expression of interest for a Bottom Collider Detector at the SSC, (May 25, 1990), p. 50.
3. Proceedings of the SLC workshop on experimental use of the SLAC collider, SLAC-247 (March, 1982), p. 158.
4. F. Sauli, Principles of operation of multiwire proportional and drift chambers, CERN 77-09 (May 3, 1977), p. 2.
5. J. Fischer et. al., Proportional chamber for very high counting rates based on gas mixtures of CF_4 with hydrocarbons, NIM A238 (1985) 249.
6. C. Lu and K.T. McDonald, Drift-chamber timing studies with a N_2 laser, DOE/ER/3072-60, June 10, 1990.
7. Private communication between C. Lu and Mark Lundin, August 8, 1990.
8. B. Jean-Marie et al., N.I.M. 159, 213 (1979).
9. F. Pius, Measurement of the longitudinal diffusion of a single electron in gas mixtures used in proportional counters, N.I.M. 205, 45 (1983).
10. B. Jean-Marie et al., Systematic measurement of electron drift velocity and study of some properties of four gas mixtures: $ArCH_4$, ArC_2H_4 , ArC_2H_6 , ArC_3H_8 , N.I.M. 159, 213 (1979).

FIGURE CAPTIONS

- 1) Geometry of the BCD Straw Tube Superlayer.
- 2) Straw Tube Detector Circuit Layout (Taken from Techniques for Nuclear and Particle Physics Experiments, W.R. Leo, p. 120).
- 3) Straw tube resolution as a function of distance from the anode. Shown are seven discriminator settings (from bottom to top: 0.01, 0.1, 0.2, 0.3, 0.4, 0.7, 1.0 volts). The amplifier is characterized in this example by a 10 ns rise time. Longitudinal diffusion has been characterized by $\sigma = 120 \mu\text{m} \sqrt{\text{Distance}(\text{cm})}$.
- 4) Mean number of ionization clusters required to trigger the discriminator trigger levels in Fig.3.
- 5) Detector efficiency for the scenario related in Fig.3 as a function of the DCA of the particle track. Shown are the efficiency values for seven discriminator settings (from top to bottom: 0.01, 0.1, 0.2, 0.3, 0.4, 0.7, 1.0 volts).
- 6) Straw drift tube spatial resolution predictions for different longitudinal diffusion factors and amplifier response rise times.
- 7) Radial electric field (V/cm) as a function of distance from the Lu-McDonald straw tube drift chamber's central wire anode (please note the suppressed zero). In addition, the drift velocity for ArC_2H_6 (50/50) is shown as a function of this field.
- 8) Pressure dependence of spatial resolution of the Lu/McDonald drift chamber filled with ArC_2H_6 (50/50).

Figure 1.

BCD STRAW TUBE SUPERLAYER

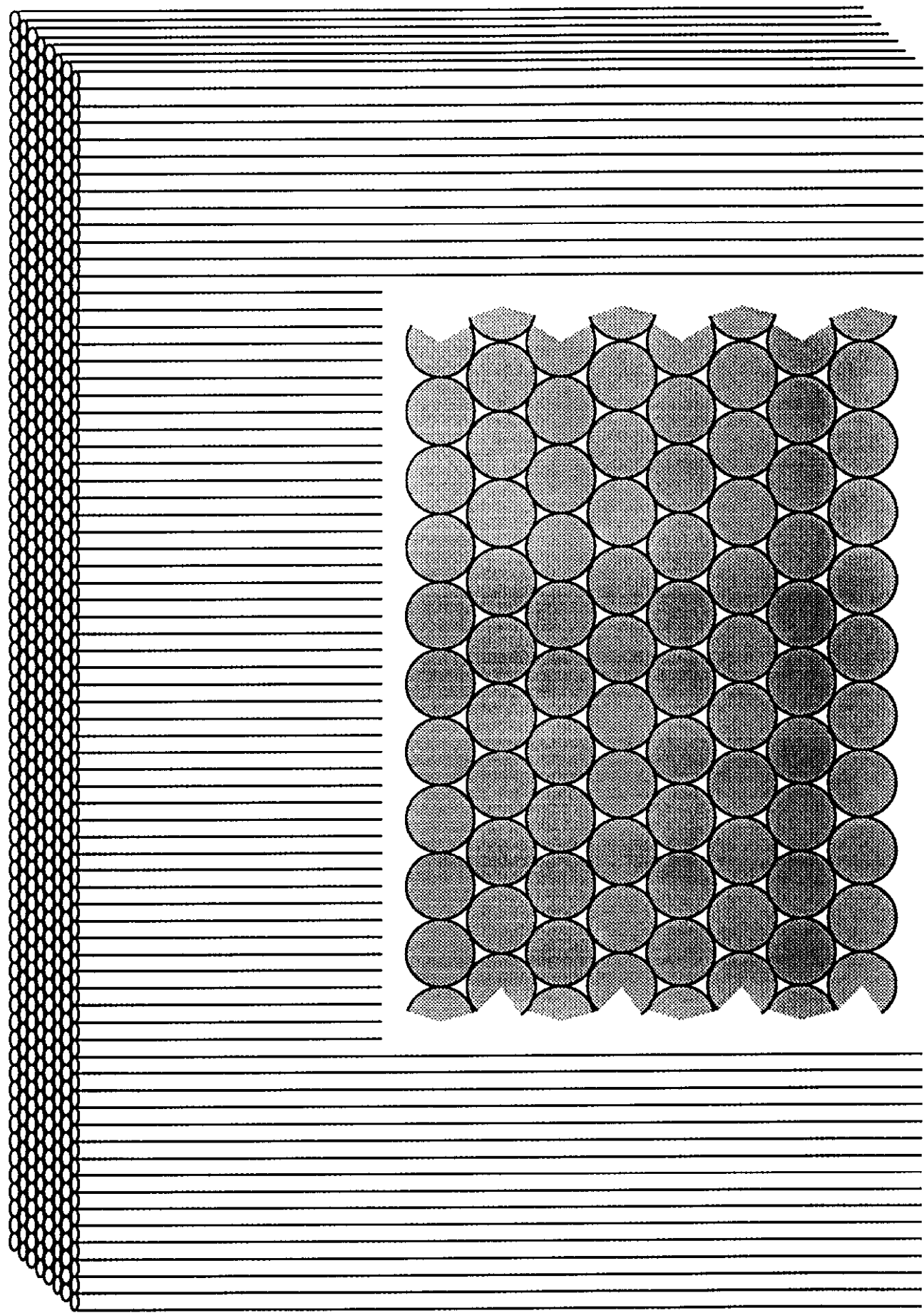


Figure 2.

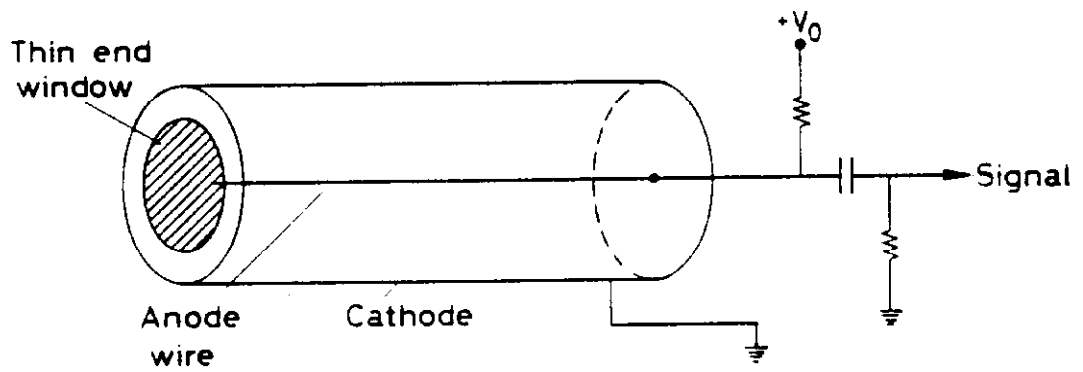


Figure 3.

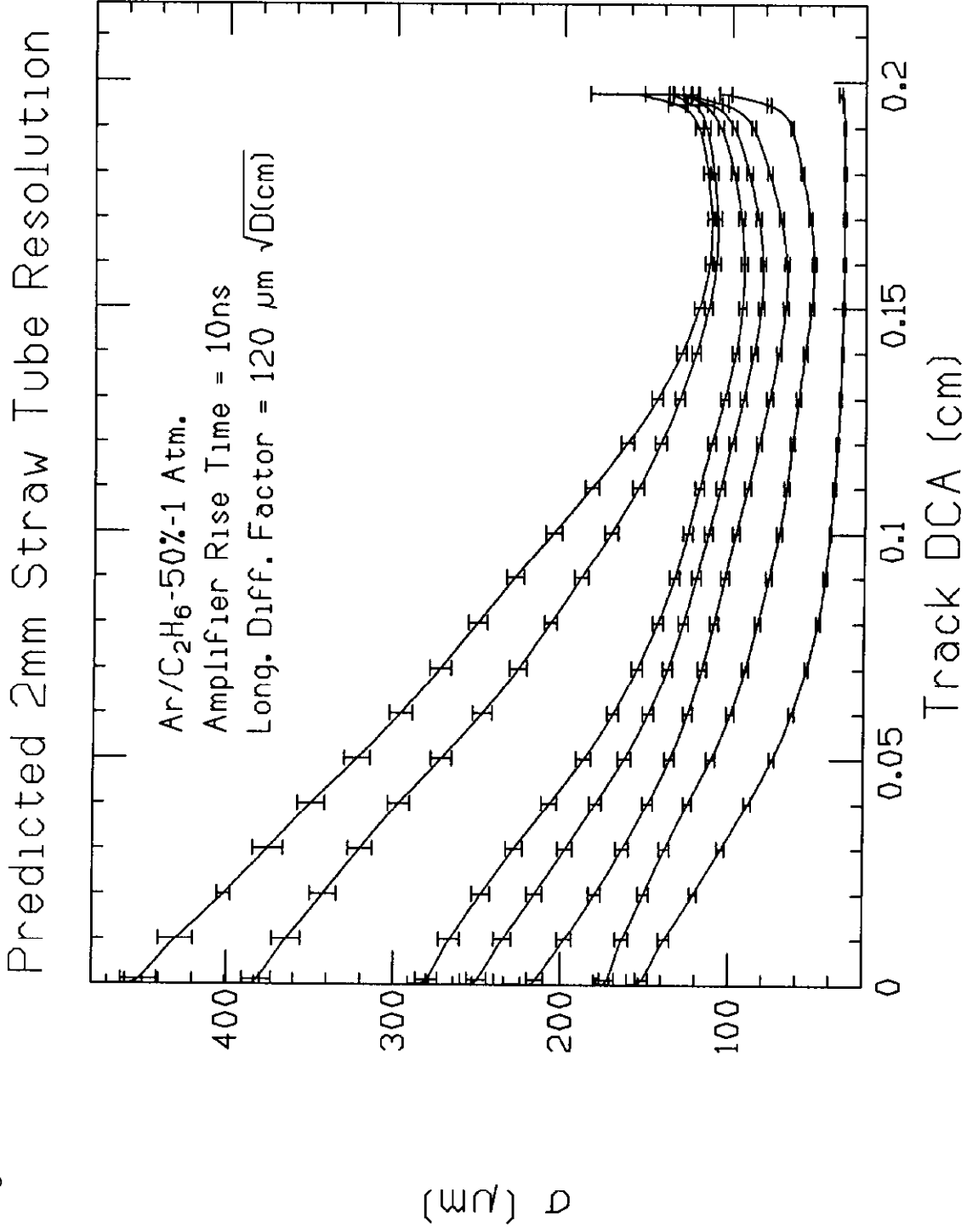


Figure 4.

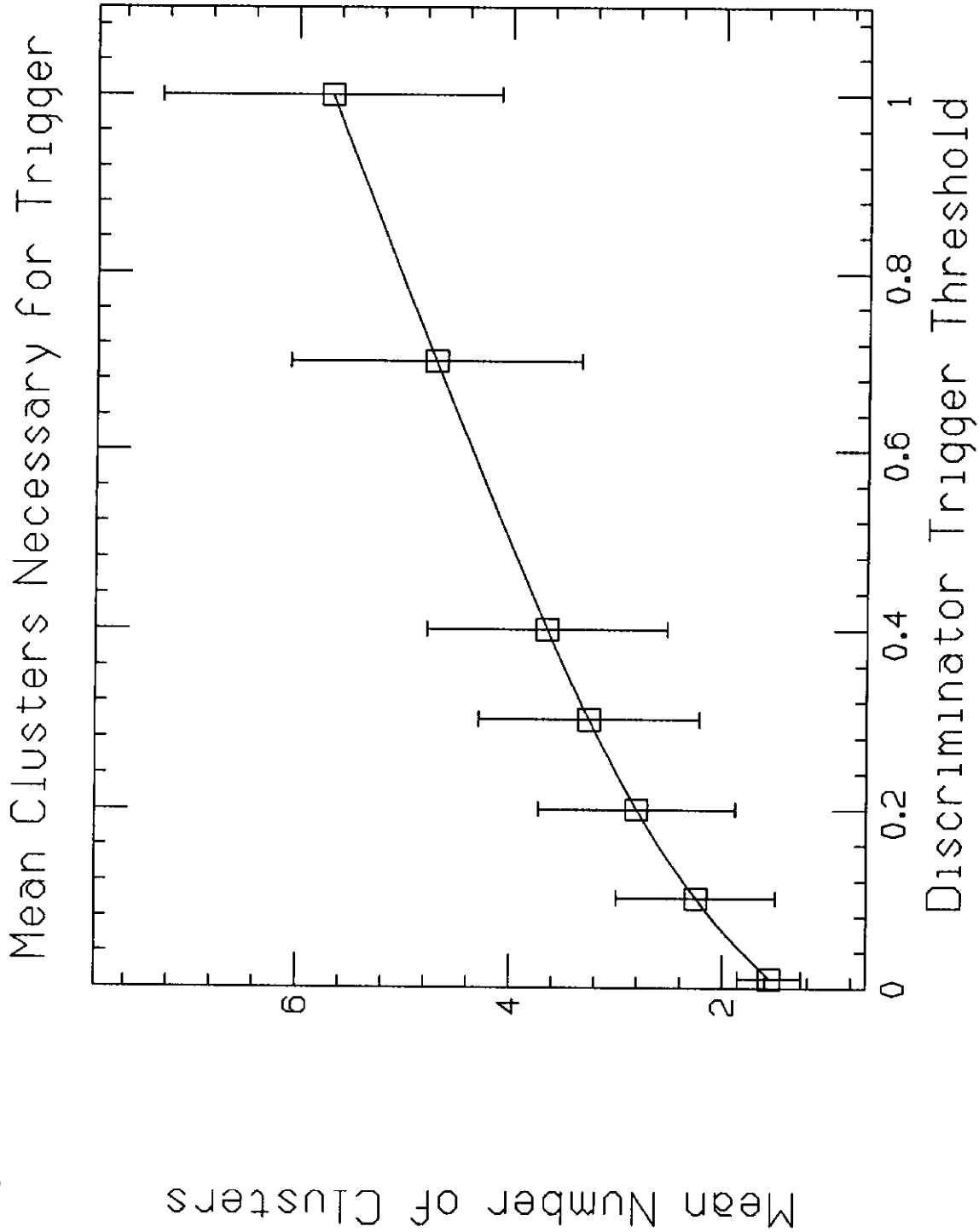


Figure 5.

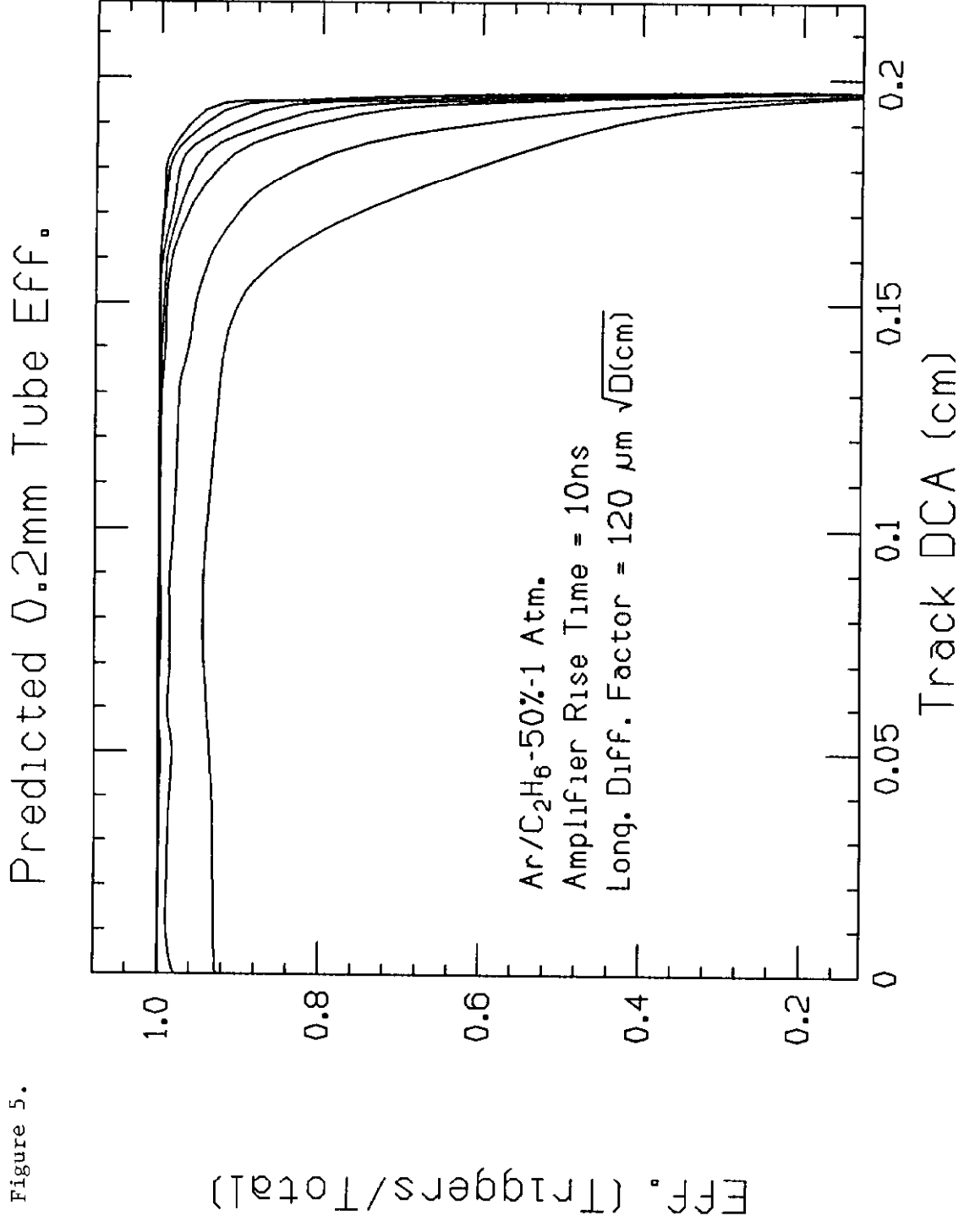


Figure 6.

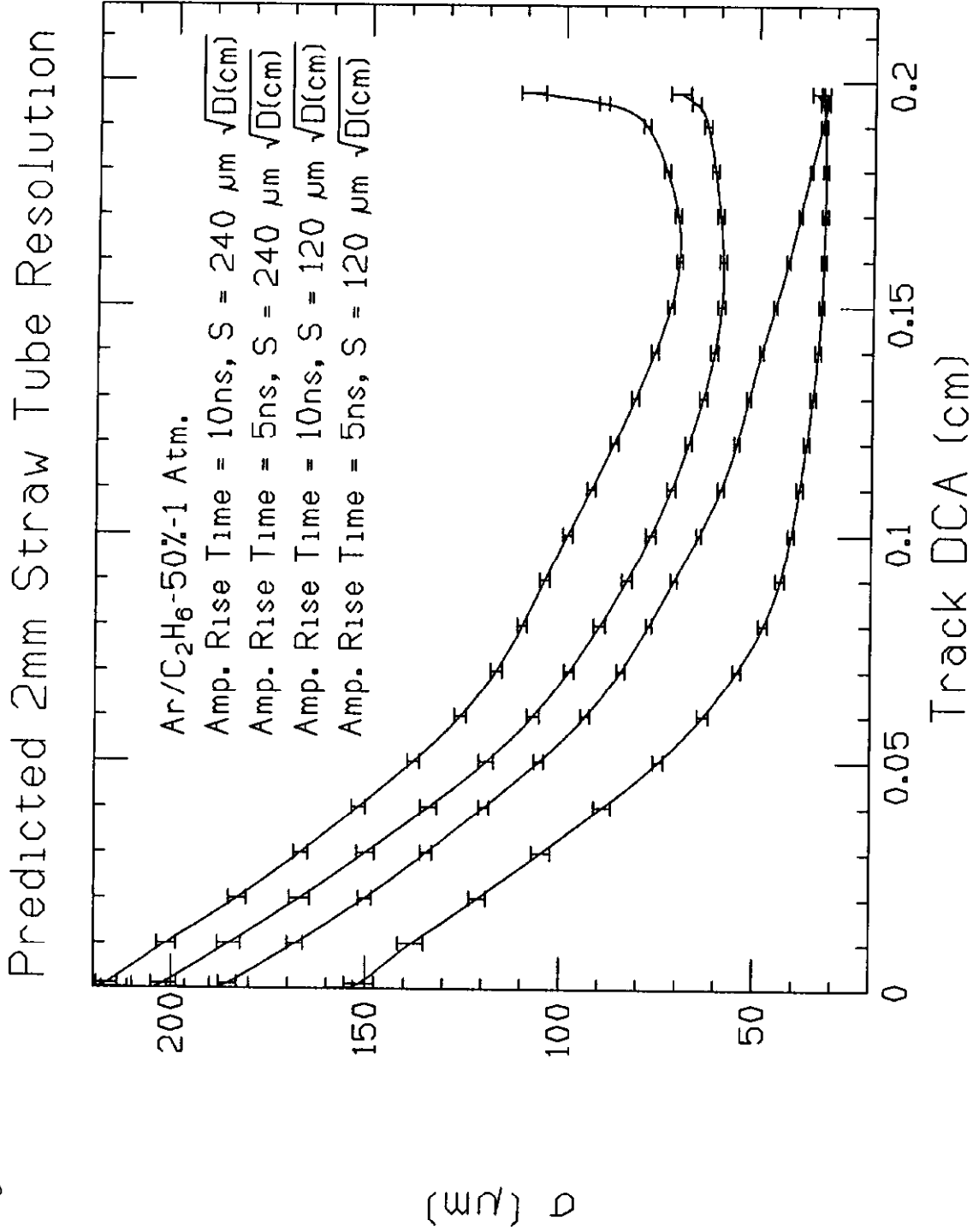
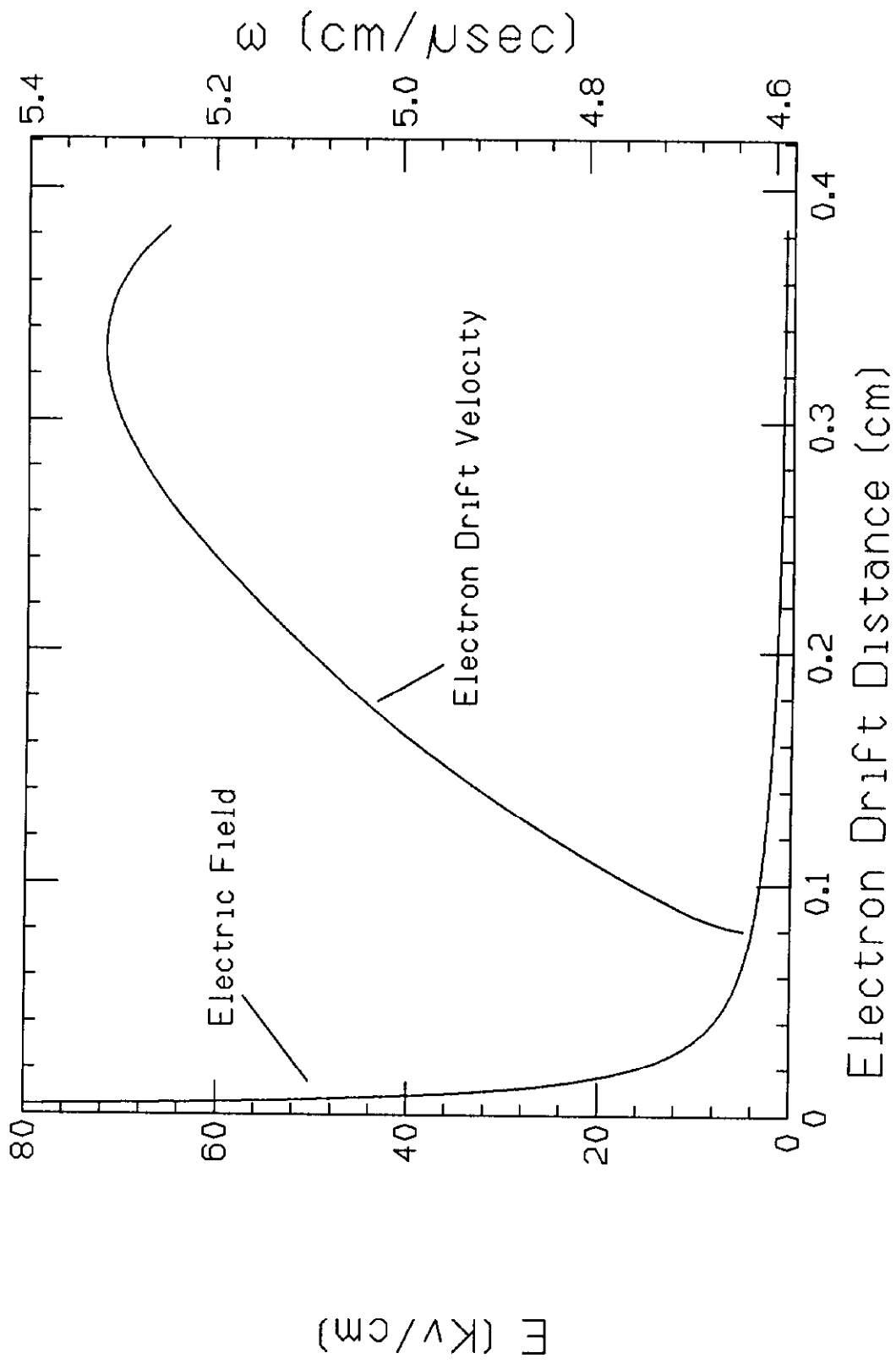


Figure 7.



Spatial Resolution of Ar/C₂H₆-50%

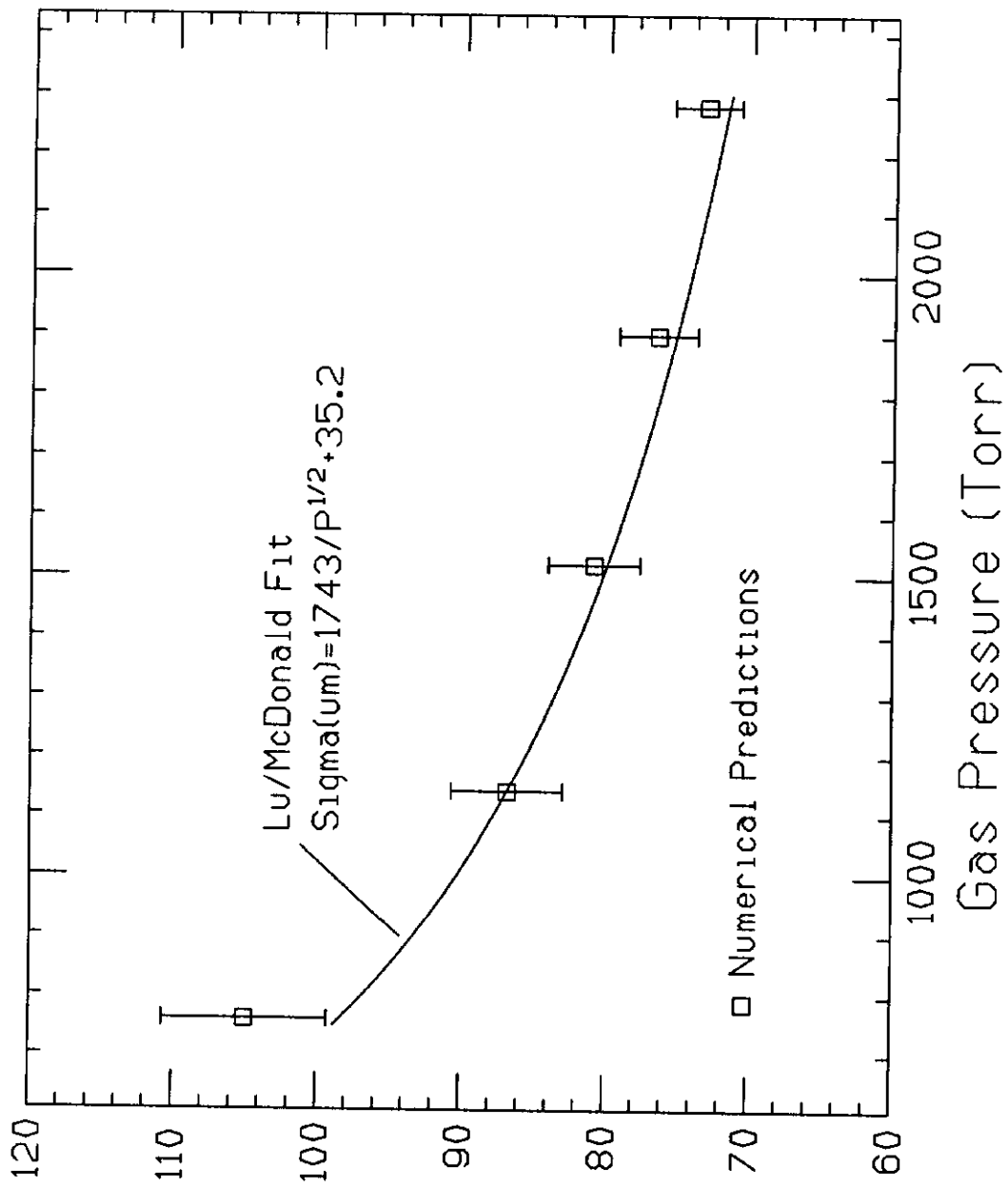


Figure 8.

Spatial Resolution (um)